SAND2011-0209C

# A negative-index metamaterial design based on metal-core, dielectric shell resonators

L. I. Basilio, L.K. Warne, W.L. Langston, W.A. Johnson, and M. B. Sinclair
Electromagnetic Effects
Sandia National Laboratories
Albuquerque, USA

***Abstract*— In this paper a simple effective-media analysis (including higher-order multipoles) is used to design a single-resonator, negative-index design based on a metal-core, dielectric-shell (MCDS) unit cell. In addition to comparing the performance of the MCDS design to various all-dielectric negative-index designs, performance trade-offs resulting from the relative positioning of the electric and magnetic modal resonances in the MCDS design are also discussed.**

***Keywords-metamaterials; negative index; core-shell; effective media***

## I. INTRODUCTION

The intent of this paper is to design a single-resonator negative-index metamaterial based on a simple effective media analysis. Unlike previous efforts in which dual-species dielectric sphere lattices (of either varying material properties or varying sizes [1,2]) have been used to realize an overlap in the magnetic resonance of one sphere with the electric resonance of the other, the design under consideration here achieves negative-index (NI) behavior by aligning the electric and magnetic responses of a single resonator. The particular structure under consideration in this paper is a spherical metal core concentric to a dielectric shell layer, as shown in Fig. 1. This structure is analogous to the dielectric-core, dielectric shell (DCDS) design presented in [3] and the performances in terms of loss and effective size can be directly compared (a preliminary comparison is given in [3]). In this paper, more extensive performance comparisons between the MCDS design and other single resonator designs are carried out (including the DCDS design). In addition, the performance (particularly in terms of loss) of the MCDS is shown to vary considerably depending on the relative positioning and amplitude of the electric and magnetic modal resonances. With the goal of moving towards "optimum" alignment between resonances (in terms of achieving low-loss NI behavior), several alignment scenarios derived from different packing fractions and ratios of metal core radius to outer shell radius are examined.

## II. EFFECTIVE MEDIA THEORY (INCLUDING HIGHER-ORDER MULTIPOLES)

The designs presented here are based on effective media theory in the form of a series of multipole-moment interactions

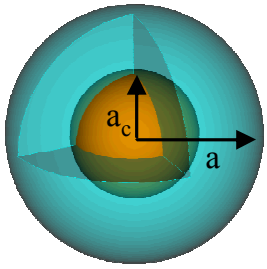


Fig. 1. A metal core dielectric shell resonator with core radius $a_c$ and dielectric shell radius $a$.

[4,5,6] which has no restrictions on the volume packing fraction $p$ (as with the Clausius-Mossotti formulation). Following an iterative matrix approach as given in [4] and enforcing continuity in $\Pi_r E_r$, $E_\Sigma$, and $E_\varphi$ at the two radial boundaries $a_c$ and $a$ (Fig. 1), the effective permittivity (or permeability by applying duality) for a lattice of MCDS spheres becomes

$$\varepsilon_e/\varepsilon_1 = 1+3p/\Lambda_e(p), \tag{1}$$

where

$$\Lambda_e(p) = -(1/R_1) - p + 1.3045R_3 p^{10/3} + 0.0723R_5 p^{14/3} - 0.5289R_3^2 p^{17/3} + 0.1526R_7 p^6 \tag{2}$$

and

$$R_n = \frac{n\varepsilon_1\left\{\left[aj_n(k_2a)\right]' + T_n\left[ah_n(k_2a)\right]'\right\} - n(n+1)\varepsilon_2\left[j_n(k_2a) + T_n h_n(k_2a)\right]}{(n+1)\varepsilon_1\left\{\left[aj_n(k_2a)\right]' + T_n\left[ah_n(k_2a)\right]'\right\} + n(n+1)\varepsilon_2\left[j_n(k_2a) + T_n h_n(k_2a)\right]} \tag{3}$$

with

$$T_n = \frac{\varepsilon_2 j_n(k_2a_c)\left[a_c j_n(k_3a_c)\right]' - \varepsilon_3 j_n(k_3a_c)\left[a_c j_n(k_2a_c)\right]'}{\varepsilon_3 j_n(k_3a_c)\left[a_c h_n(k_2a_c)\right]' - \varepsilon_2 h_n(k_2a_c)\left[a_c j_n(k_3a_c)\right]'} e^{\left\{ik-|\mathrm{Im}(k_2)|\right\}(a-a_c)}. \tag{4}$$

Here $a_c$ is the metal core radius, $a$ is the outer radius of the dielectric shell, $p = 4\pi a^3/(3b^3)$, while $\Pi_1$, $\Pi_2$, and $\Pi_3$ represent the permittivity of the host, shell, and core materials, respectively. The wavenumbers $k$ appearing in (3) and (4) are

given by $\gamma(\mu\Pi)^{1/2}$ where the subscripts indicate the corresponding sphere region (shell or core) and $\gamma$ is the radial frequency. Note that in the case of a conducting core, as is the main focus of this paper, the core permittivity is taken as $\Pi_3 = \Pi_0 + i(\alpha/\gamma)$, where $\alpha$ is the metal conductivity (an $e^{-i\gamma t}$ is assumed throughout).

## III. RF MCDS DESIGN EXAMPLES

In this section a variety of RF negative index MCDS designs is presented. Although a metal core of $\alpha = 5.7e7$ *S/m* and a dielectric shell of relative permittivity $\Pi_{2r} = 100 + i0.1$ is common to all the RF designs (a lossless design is also included for comparison), the ratio of core to shell radius is varied in each case. This parameterization study is conducted for the purposes of understanding how the relative positioning between the MCDS electric and magnetic modes (in frequency) affects the loss performance of the negative index behavior. It is significant to note that the frequency alignment between the electric and magnetic resonance can be critical in obtaining low-loss degenerate resonator designs (MCDS, DCDS), as well as low-loss dual-species resonator designs (such as split-ring-resonators and a loaded-dipole designs).

### A. Negative Index, Packing Fraction Independent Design

As an initial step to the design of an MCDS resonator, electric and magnetic modal degeneracy (of the first electric and first magnetic modes) is enforced when the resonator is taken to be lossless (perfectly-electrically conducting (PEC) core with a purely real $\Pi_{2r}$ shell layer). Proceeding in this manner, a simple transcendental equation governing the ratio of core radius to outer shell radius ($R$) is found to be

$$\tan\left(R^{-3/2} - R^{-1/2}\right) + R^{-1/2} = 0, \qquad (5)$$

with a corresponding resonant frequency $ka = R^{-3/2}$. Solving (5) results in $R = a_c/a = 0.418740$ and a degenerate resonance of $ka = 3.690484$. It is significant to note that this resonance is shifted upward from the first magnetic position $ka = \pi$ of a non-layered sphere resonator but is still below the non-layered first electric position of $ka = 4.49$.

The degeneracy of the electric and magnetic mode for a lossless MCDS design (with $R = 0.419$) is demonstrated in Fig. 2 where the peaks in the effective media permittivity and permittivity coincide at approximately 2.8 GHz. (It is significant to note that, since (5) is derived assuming a single isolated MCDS resonator, a low packing fraction of $p = 0.1$ has been assumed in the effective media calculations.) As expected, leakage of the magnetic mode into the outside region of the MCDS cavity resonator results in a wider-band response in the effective permeability than for the effective permittivity and thus, the negative region of the permittivity is absorbed into the region of negative permeability.

Fig. 2 also shows effective media results when $R$ is taken to be 0.419 but loss is now added to the metal core ($\alpha = 5.7e7$ *S/m*) and the shell is taken to have a permittivity of $\Pi_{2r} = 100 + i0.1$. Although the loss reduces the peak levels in the real parts of both $\Pi_e$ and $\mu_e$, Fig. 2 demonstrates that modal degeneracy is preserved for this lossy MCDS design. The loss performance of various MCDS designs (including this one) is described in the next section.

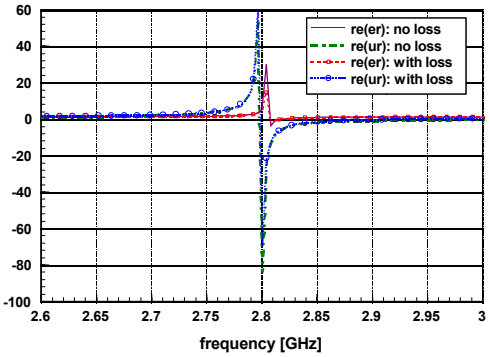


Fig. 2. The real part of the relative effective permittivity and permeability for a MCDS shell design with core of radius $a_c$ = 2.9 mm and a dielectric shell of with radius a = 6.2 mm. A volume packing fraction of p = 0.1 is assumed.

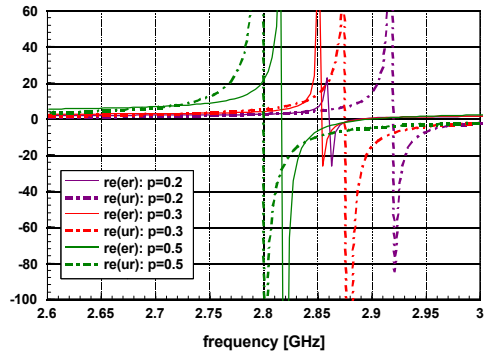


Fig. 3. The real part of the relative effective permittivity and permeability for a MCDS shell design with core of radius $a_c$ = 2.6 mm and a dielectric shell of with radius a = 6.2 mm. Volume packing fractions of p = 0.5, 0.3, and 0.2 are included.

### B. Varying the Ratio of Core Radius to Outer Sphere Radius

While in the previous subsection (5) was used to arrive at a simple preliminary design ($R = 0.419$ yielding the same resonant frequency for the first electric and magnetic mode), in this section the value of is $R$ is varied so as to ultimately understand what type of frequency alignment between resonances yields the best NI loss performance.

Using the results of (5) as a starting value, the value of $R$ is perturbed to 0.342 and 0.467 [3]. In comparing these designs, it is most significant to note that only the original $R = 0.419$ design demonstrates NI behavior over the packing fraction range from nearly touching ($p = 0.5$) to nearly isolated ($p = 0.1$). (Increasing neighbor interactions resulting from higher packing perturbs the peak alignment seen in Fig. 2, but overlap in the negative region of the permittivity and permeability still occurs.) The effect of packing on the positions of the electric and magnetic resonances is demonstrated for the case of $R = 0.467$ in Fig. 3. It is clear that as the packing fraction is increased both the magnetic and electric modes demonstrate boosted responses and both shift towards lower frequencies (with the magnetic resonance being

more sensitive to interaction effects and exhibiting larger shifts). In addition, while the negative-size zero-crossing of the electric response remains relatively fixed, the magnetic mode zero crossing (negative-side) is pushed out to higher frequencies as a result of the increase amplitude response associated with the higher packing cases (although not visible for the *x*-axis range in Fig. 3). The significance of these effects is that for packing fractions greater than approximately 0.3 overlap between the negative regions of the permittivity and permeability occurs. (Note that for $p \leq 0.2$, a NI behavior is not realized). The effective media parameters for the $R$ = 0.342 case are not included here but are observed to demonstrate similar behavior to the $R$ = 0.467 design as the packing fraction varies (however, overlap in the negative portions of the effective media curves begins to occur at $p$ = 0.2). Thus, it is important to note that, with the exception of the $R$ = 0.419 design, the alternative MCDS arrangements must rely on interaction effects (ie. higher packing fractions) to realize NI behavior.

With the goal of identifying low-loss MCDS designs, the overall performance of the $R$ = 0.419 is next evaluated for a variety of packing fractions. As discussed previously, alignment between peaks (negative) in the effective media parameters occurs for the low packing fraction case (by design) but, as one would expect, this alignment is perturbed as $p$ increases. The result of this shifting in resonances is demonstrated in Table 1, where the bulk attenuation is seen to decrease as the packing fraction is increased (the attenuation is given in terms of dB/$\varsigma_0$ for a real part of the effective refractive index approximately equal to —1 in all cases). This is not too surprising, as moving the resonators closer together results in amplified responses and ultimately overlap in the tail portions of the negative permittivity and negative permeability curves, rather than in coincident peaks (as for $p$ = 0.1). In addition to a loss measure for each packing fraction instance (dB/$\varsigma_0$), Table 1 also presents the corresponding figure-of-merit ($FOM = real(n_{eff})/imag(n_{eff})$) and the effective lattice spacing (given in terms of the effective wavelength ($b/\varsigma_{eff}$) and the free-space wavelength ($b/\varsigma_0$)) for each of the designs. Table 1 demonstrates that these MCDS designs are characterized by reasonable values of loss (perhaps competitive or better to split-ring/rod-type structures due to the smooth shape of the metal core) and also stay well within the homogenization limit in terms of their effective size ($b/\varsigma_{eff}$ and $b/\varsigma_0$ are both much less than 0.5). Since it can analytically be shown that overlap between the lowest-order electric and magnetic mode of a DCDS resonator is not possible, the MCDS design (which relies on lowest-order modal overlap) has a clear size advantage of over its all-dielectric counterpart. (The DCDS design in [3] realizes negative-index behavior with overlap of the second resonances). On the other hand, due to the metallic nature of the core of the MCDS design, the advantage in terms of loss goes to the DCDS configuration.

TABLE I. PERFORMANCE SUMMARY OF R = 0.419 MCDS DESIGN

| **R = 0.419** | **p = 0.1** | **p = 0.2** | **p = 0.3** | **p = 0.5** |
|---|---|---|---|---|
| **f [GHz]** | 2.82 | 2.82 | 2.82 | 2.8 |
| **$n_{eff}$** | (—0.947,0.20) | (—1.46,0.073) | (—1.17,0.05) | (—1.17,0.035) |
| **FOM** | —4.7 | —20.0 | —23.5 | —33.4 |
| **dB/$\varsigma_0$** | —10.9 | —4.0 | —2.7 | —1.9 |
| **$b/\varsigma_{eff}$** | 0.20 | 0.23 | 0.16 | 0.20 |
| **$b/\varsigma_0$** | 0.20 | 0.16 | 0.14 | 0.20 |

It is important to point out that although the $R$ = 0.419 demonstrates NI behavior over the full range of packing, it is the $R$ = 0.342 case (smallest core) which demonstrates the best loss performance of the three $R$ designs. (However, this can be said only for a restricted set of packing fractions for which the $R$ = 0.342 and $R$ = 0.467 designs realize a NI region.) Alternatively, the loss performance for a given $R$ design improves as the packing fraction increases (since, as discussed previously, overlap in the tail regions of the negative permittivity and negative permeability occurs and is pushed further away from the peak losses with increased packing).

## IV. PERFORMANCE SURVEY OF VARIOUS INFRARED NEGATIVE-INDEX DESIGNS

Reasonable loss performance for an RF MCDS design was demonstrated in the previous section. However, since it is also of interest to compare the performance of the MCDS design to the performance of alternative designs as the frequency increases and loss effects become even more significant, in this section a mid-infrared (IR) MCDS is presented. The performance of this design (in terms of *FOM*, bulk attenuation, and effective size) is then compared to a DCDS design, as well as a dielectric-core, polaritonic shell (DCPS) design (both designed for IR). The effective media characterization for each of these designs is derived directly from the analysis given in Section II. A dielectric of lead telluride (PbTe) with $\Pi_r = 32.04 + i0.0524$ [7] (for the shell in the MCDS design and the core in the remaining designs) and a packing fraction of $p = 0.3$ is assumed throughout.

### *A. Infrared MCDS Design Example*

Assuming a gold (Au) core and a ratio of core radius to outer shell radius of 0.342 ($R = a_c/a$ is selected based on the previous results), (1) was used to identify the core radius that yielded an effective refractive of approximately —1 at approximately 10 μm. It is important to note that the dispersive properties of Au in this frequency band were accounted for by incorporating Sandia National Laboratories microfab data into $\Pi_3 = \Pi_3(\varsigma)$ in (4). One MCDS prototype satisfying the design specifications (within a constrained design space defined by 0.1 μm ≤ $a_c$ ≤ 2 μm) is given by $a$ = 1.06 μm and its design performance is summarized in Table 2. Although the loss performance associated with the highly dispersive Au core is not particularly good (though still competitive or better than many IR SRR/dipole designs), it is

TABLE II. PERFORMANCE SUMMARY OF IR CORE-SHELL DESIGNS

| | $\varsigma_o$ | $n_{eff}$ | FOM | $dB/\varsigma_o$ | $b/\varsigma_{eff}$ | $b/\varsigma_o$ |
|---|---|---|---|---|---|---|
| **MCDS** | 10.68 | (—1.02,0.471) | —2.2 | —25.7 | 0.27 | 0.24 |
| **DCDS** | 10.0 | (—1.02,0.041) | —24.9 | —2.2 | 0.68 | 0.66 |
| **DCPS** | 9.68 | (—0.995,0.397) | —2.5 | —21.6 | 0.31 | 0.29 |

apparent that the MCDS design has a significant advantage in terms of the electrical size of the lattice ($b/\varsigma$) and thus stays well within the metamaterial homogenization limit.

### *B. Infrared DCDS Design Example*

For this design example, the remaining parameters in (1)-(4) are varied (a PbTe core and $p$ are fixed) so that a "high-quality", $real(n_{eff}) \approx -1$ DCDS design is realized. In this case "high-quality" is being defined as one of the lowest loss and electrically smallest solutions (several comparable solutions exist) identified within a design space constrained to 0.1 μm ≤ $a_c \le 5$ μm, 0.11 μm ≤ $a \le 10$ μm, and $2 \le real(\Pi_{2r}) \le 20$. The results for the selected design, $a$ = 2.75 μm and $\Pi_{2r} = 5.2 + i0.009$, are presented in Table 2. (The loss tangent for the shell permittivity has been assumed to be the same as for PbTe). As previously mentioned, the DCDS realizes NI behavior by relying on overlap between the second electric and magnetic resonances (as opposed to the lowest-order resonances for the MCDS design). This is demonstrated with the effective refractive index for the selected DCDS design shown in Fig. 4, where the lowest-order resonances yield non-degenerate peaks in $n_{eff}$ but remain positive until reaching the degenerate second-order modes at a lower wavelength. The effect of pushing the overlap to lower wavelength is evident in Table 2, where the lattice constant $b$ is seen to go beyond 0.5 wavelengths. Clearly the advantage of this designs lies in its very low-loss NI performance.

### *C. Infrared DCPS Design Example*

One alternative to the DCDS design, which is not dependent on the overlap of resonances, is a dielectric-core, polaritonic shell design (DCPS). With this structure, the magnetic resonance of the dielectric core (in this case PbTe) is overlayed on the negative permittivity (non-resonant) response associated with the polaritonic shell layer so that a $n_{eff} \approx -1$ results at approximately 10 μm. For this particular example, a silicon carbide (SiC) shell of $\Pi_{2r} = -0.580 + i0.116$ was taken as a fixed parameter and a search within the same design space to that in the previous section was performed. (The SiC permittivity value was again extracted from Sandia microfab data.) The results for a candidate DCPS design given by $a_c$ = 0.87 μm and $a$ = 1.16 μm are included in Table 2. The DCPS

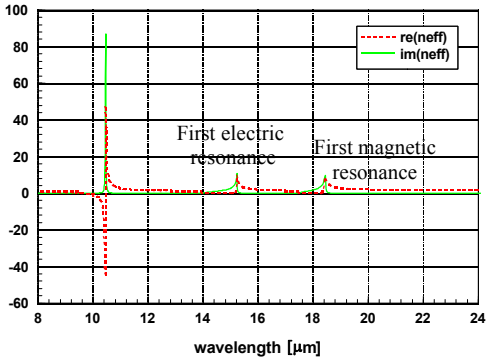


Fig. 4. The effective refractive index for a DCDS shell design with radii $a_c$ = 1.45 μm, a = 2.75 μm and a dielectric shell permittivity $\Pi_{2r} = 5.2 + i0.009$.

design is significantly smaller than the DCDS structure and falls in between the alternative designs in terms of its loss performance (though only slightly better than the MCDS design and not nearly as good as the DCDS design).

## V. SUMMARY

In this paper, a higher-order multipole effective media analysis for core-shell spherical resonators was presented and applied to the design of negative-index metamaterials based on metal-core, dielectric shell resonators, as well as dielectric-core, dielectric shell resonators (polaritonic shells were also considered). The performance of various candidate designs within each of these categories was evaluated and a preliminary study of the advantages, disadvantages, and tradeoffs between the designs was carried out.

## REFERENCES

[1] A. Ahmadi and H. Mosallaei, "Physical configuration and performance modeling of all-dielectric metamaterials", Phys. Rev. B, vol. 77, art. 045104, 2008.

[2] L. Jylha, I. Kolmakov, S. Maslovski, and S. Tretyakov, "Modeling of isotropic backward-wave materials composed of resonant spheres", J. Appl. Phys., vol. 99, art. 043102, 2006.

[3] E. Kuester, N. Memic, S. Shen, and A. Scher, "A negative refractive index composite medium based on a cubic array of layered nonmagnetic spherical particles," unpublished..

[4] J. Lam, "Magnetic permeability of a simple cubic lattice of conducting magnetic spheres", J. Appl. Phys., 60 (12), p. 4230-4235, 1986. .

[5] P. Waterman and N. Pederson, "Electromagnetic scattering by periodic arrays of particles", J. Appl. Phys., vol. 49, p. 2609-2618, 1986.

[6] L. Basilio, L. Warne, W. Johnson, W. Langston, and M. Sinclair, "An infrared negative-index layer based on single-species particles in a polaritonic host", unpublished.

[7] E. Palik, Handbook of Optical Constants and Solids, Academic, Orlando, Fla., 1985.